Preparation and Characterization of Quantum Size Zinc Oxide: A Detailed Spectroscopic Study

Detlef W. Bahnemann,† Claudius Kormann, and Michael R. Hoffmann*

W. M. Keck Laboratories, California Institute of Technology, Pasadena, California 91125
(Received: November 5, 1986; In Final Form: March 18, 1987)

We report the synthesis of transparent colloidal suspensions of small zinc oxide particles in water, 2-propanol, and acetonitrile. Quantum (Q)-size effects are observed during particle growth and qualitatively interpreted by using a simple molecular orbital (MO) picture. The particles at the final stage of growth are approximately spherical in shape and consist of 2000–3000 ZnO molecules. They exhibit many of the photophysical properties of bulk zinc oxide. However, pronounced shifts in the absorption spectrum during the illumination of anoxic suspensions of ZnO reveal a distinctively different behavior of these small particles. Fluorescence spectra of the ZnO sols suggest that adsorbed electron relays are necessary to shuttle electrons from the conduction band into lower lying traps. Two fluorescence maxima are observed at the final growth stage of the ZnO particles. The bandgap fluorescence at 365 nm has an extremely short lifetime ($\tau < 100$ ps), while the visible luminescence at 520 nm exhibits a slower biexponential decay (i.e., $\tau = 14$ and 190 ns). The latter fluorescence is attributed to photogenerated electrons tunneling to preexisting, trapped holes. The low overall fluorescence quantum yield of $\Phi = 0.03$ measured in these zinc oxide suspensions is indicative of radiationless transitions accompanying the emissions. A pronounced pH dependence of the Stern–Volmer constants obtained with various ionic substances, that effectively quench the 520-nm emission, is explained by specific adsorption to the charged particle surface. The zero point of charge (pH_{zpc}) of the aqueous colloidal suspension was determined to be 9.3 ± 0.2 by several independent methods.

Introduction

The photoelectrochemistry of small semiconductor particles has been an area of active research.[1-3] Recently, there has been a growing interest in ultrasmall particles[4-28] that fall into the transition range between molecular and bulk properties (i.e., with diameters from 1 to 10 nm).[4] Bulk semiconductors exhibit a pronounced increase in light absorption when photon energies exceed the bandgap energy (E_g); however, the photophysics of ultrasmall semiconductor particles is substantially different. Quantum mechanical calculations[4-6] and experimental observations[7-28] suggest that the energy level of the first excited state of the exciton increases with decreasing particle size thus leading to a blue shift in the absorption spectrum. Particle growth results in spectral shifts from an absorption onset (λ_{os}) in the UV for dimers and oligomers to a λ_{os} for the bulk material in the visible or near-IR. In several cases, a concomitant shift in the visible fluorescence (i.e., with $\lambda_{em} > \lambda_{os}$) has been noted.[14-17,19,21] Koch et al.[21] have reported a shift of the onset of absorption of ZnO colloids from 310 to 360 nm during particle growth in 2-propanol, while at the same time the maximum of the fluorescence peak shifted from 460 to 540 nm. Their paper also describes the preparation of an aqueous colloidal suspension of ZnO which, however, requires the presence of a colloid stabilizer, e.g., hexametaphosphate.[21]

α-Fe_2O_3,[29-31] WO_3,[32] and TiO_2[33-35] can be synthesized as transparent colloids in water; however, synthesis of ZnO in H_2O is not readily achieved (e.g., $\Delta G_f° = -0.39$ kJ mol^{-1} for reaction 1 at 25 °C; $\Delta G_f° = -2.79$ kJ mol^{-1} at 100 °C, $\Delta G_f° = 0$ at 13 °C).[36]

$$Zn(OH)_2 \rightleftharpoons ZnO + H_2O \qquad (1)$$

Furthermore, Schindler et al.[37-39] have shown that the dissolution rate of ZnO increases with decreasing particle size. In this respect we report a novel method for the synthesis of transparent ZnO colloids that are stable both in organic and in aqueous suspensions in the absence of stabilizers. In addition, we provide an analysis of the dynamic changes in spectral properties of transparent colloidal suspensions of ZnO that take place during particle growth.

Crystalline ZnO exhibits a characteristic fluorescence spectrum with two maxima around 380 and 500 nm.[40-51] The emission at $\lambda_{em} = 380$ nm has been attributed to the exciton band;[44,51] however, no conclusive interpretation for the visible fluorescence

† Permanent address: Bereich Strahlenchemie, Hahn-Meitner Institut Glienicker Strasse 100, D1000 Berlin 39, West Germany.

(1) Grätzel, M. *Acc. Chem. Res.* **1981**, *14*, 376.
(2) Fendler, J. H. *J. Phys. Chem.* **1985**, *89*, 2730.
(3) Bockris, J. O'M.; Dandapani, B.; Cocke, D.; Ghoroghchian, J. *Int. J. Hydrogen Energy* **1985**, *10*, 179.
(4) Brus, L. E. *J. Phys. Chem.* **1986**, *90*, 2555.
(5) Brus, L. E. *J. Chem. Phys.* **1983**, *79*, 5566.
(6) Brus, L. E. *J. Chem. Phys.* **1984**, *80*, 4403.
(7) Ekimov, A. I.; Onushchenko, A. A. *JETP Lett.* **1981**, *34*, 345.
(8) Ekimov, A. I.; Onushchenko, A. A. *JETP Lett.* **1984**, *40*, 1136.
(9) Ekimov, A. I.; Efros, Al. L.; Onushchenko, A. A. *Solid State Commun.* **1985**, *56*, 921.
(10) Rossetti, R.; Nakahara, S.; Brus, L. E. *J. Chem. Phys.* **1983**, *79*, 1086.
(11) Rossetti, R.; Ellison, J. L.; Gibson, J. M.; Brus, L. E. *J. Chem. Phys.* **1984**, *80*, 4464.
(12) Rossetti, R.; Hull, R.; Gibson, J. M.; Brus, L. E. *J. Chem. Phys.* **1985**, *82*, 552.
(13) Rossetti, R.; Hull, R.; Gibson, J. M.; Brus, L. E. *J. Chem. Phys.* **1985**, *83*, 1406.
(14) Chestnoy, N.; Harris, T. D.; Hull, R.; Brus, L. E. *J. Phys. Chem.* **1986**, *90*, 3393.
(15) Weller, H.; Koch, U.; Gutiérrez, M.; Henglein, A. *Ber. Bunsen-Ges. Phys. Chem.* **1984**, *88*, 649.
(16) Fojtik, A.; Weller, H.; Koch, U.; Henglein, A. *Ber. Bunsen-Ges. Phys. Chem.* **1984**, *88*, 969.
(17) Weller, H.; Fojtik, A.; Henglein, A. *Chem. Phys. Lett.* **1985**, *117*, 485.
(18) Fischer, Ch.-H.; Weller, H.; Fojtik, A.; Lume-Pereira, C.; Janata, E.; Henglein, A. *Ber. Bunsen-Ges. Phys. Chem.* **1986**, *90*, 46.
(19) Fojtik, A.; Weller, H.; Henglein, A. *Chem. Phys. Lett.* **1985**, *120*, 552.
(20) Baral, S.; Fojtik, A.; Weller, H.; Henglein, A. *J. Am. Chem. Soc.* **1986**, *108*, 375.
(21) Koch, U.; Fojtik, A.; Weller, H.; Henglein, A. *Chem. Phys. Lett.* **1985**, *122*, 507.
(22) Weller, H.; Schmidt, H. M.; Koch, U.; Fojtik, A.; Baral, S.; Henglein, A.; Kunath, W.; Weiss, K.; Dieman, E. *Chem. Phys. Lett.* **1986**, *124*, 557.
(23) Henglein, A.; Kumar, A.; Janata, E.; Weller, H. *Chem. Phys. Lett.* **1986**, *132*, 133.
(24) Tanaka, T.; Iwasaki, M. *J. Photogr. Sci.* **1983**, *31*, 13.
(25) Tanaka, T.; Iwasaki, M. *J. Imaging Sci.* **1985**, *29*, 86.
(26) Itoh, T.; Kirihara, T. *J. Lumin.* **1984**, *31&32*, 120.
(27) Nozik, A. J.; Williams, F.; Nenadović, M. T.; Rajh, T.; Micić, O. I. *J. Phys. Chem.* **1985**, *89*, 397.
(28) Sandroff, C. J.; Hwang, D. M.; Chung, W. M. *Phys. Rev. B* **1986**, *33*, 5953.
(29) Stramel, R. D.; Thomas, J. K. *J. Colloid Interface Sci.* **1986**, *110*, 121.
(30) Penners, N. H. G.; Koopal, L. K. *Colloids Surf.* **1986**, *19*, 337.
(31) Bahnemann, D. W.; Kern, J.; Hoffmann, M. R., manuscript in preparation.
(32) Suda, H.; Imai, N. *J. Colloid Interface Sci.* **1985**, *104*, 204.
(33) Duonghong, D.; Ramsden, J.; Grätzel, M. *J. Am. Chem. Soc.* **1982**, *104*, 2977.
(34) Bahnemann, D.; Henglein, A.; Lilie, J.; Spanhel, L. *J. Phys. Chem.* **1984**, *88*, 709.

0022-3654/87/2091-3789$01.50/0

peak has been given previously.[43,45-50] A detailed study of the fluorescence behavior of the zinc oxide sols thus affords further insight into its mechanism.

Experimental Section

Chemicals and solvents were of reagent grade and used without further purification. The water employed in all preparations was purified by a Milli-Q/RO system (Millipore) resulting in a resistivity of >18 MΩ cm. Reflectance spectra of powder samples with $BaSO_4$ as a reference were obtained with a Shimadzu MPS-2000 spectrophotometer equipped with an integrating sphere. The same instrument and a HP 8451A diode array spectrophotometer were used to measure UV/vis absorption spectra. Fluorescence spectra were recorded using a Shimadzu RF 540 spectrofluorometer. Appropriate filters to avoid second-order contributions were installed in the excitation and emission light paths. Fluorescence quantum yields were measured with 6×10^{-5} M quinine sulfate in 1 N H_2SO_4 as a reference standard.[52] All steady-state spectra were measured at 25 °C.

Particle sizes were determined by transmission electron microscopy (TEM). To prepare the TEM samples a drop of the colloidal suspension was applied for 30 s to a copper mesh covered with a carbon film and subsequently removed with a paper tip. Adhesion of the particles was promoted by exposing the carbon film to a glow discharge prior to this procedure.

The irradiation apparatus consisted of an Osram XBO 450-W xenon lamp in a Müller LX 1450-2 lamp housing and a GM 252 (Kratos) monochromator with the appropriate UV filters. Actinometry was performed with (*E*)-2-(2,5-dimethyl-3-furylethylidene)(isopropylidene)succinic anhydride in toluene according to the method of Heller.[53]

In order to assess the fluorescence yield of the colloidal suspensions under various oxygen partial pressures 3-mL aliquots were bubbled for 20 min with an O_2/N_2 gas mixture. While recording the fluorescence spectra, the suspensions were kept silent being still covered by the O_2/N_2 atmosphere. Since prolonged agitation of the aqueous sols leads to coagulation of the colloid (the isopropanolic colloid is found to be more stable), fresh samples were prepared for each measurement. In order to determine the dependency of the fluorescence yield on the H_2O_2 concentration for oxygen free suspensions, 3-mL aliquots containing calibrated amounts of H_2O_2 were subjected to at least three freeze–pump–thaw cycles ($p \leq 10^{-5}$ Torr) before the measurement.

Fluorescence decay times were measured in collaboration with Douglas Magde at the University of California, San Diego. Details of the experimental setup have been described elsewhere.[54] Colloidal suspensions of ZnO in 2-propanol or in water were excited with short laser pulses (≤10 ps) at 330 nm and the fluorescence decays were followed at 365 nm and at 520 nm. It was ascertained by the use of small pulse energies (with $\simeq 10^6$ photons/pulse absorbed in a volume $\geq 10^{-5}$ cm^3) that the absorbed photon number per pulse did not exceed a thousandth of the ZnO particle concentration; 4×10^9 pulses were averaged in each experiment.

Various compounds, i.e., organic or inorganic anions or cations, were examined as quenchers of the emission. Stern–Volmer-type plots were used to analyze data relating the fluorescence intensity of a sol containing a known concentration of quenching agent to the intensity of a pure colloidal sol. The excitation wavelength was 330 nm.

Preparation of Colloidal ZnO in 2-Propanol, Water, and Acetonitrile. For a typical preparation 1 mmol of $Zn(OAc)_2$ (zinc acetate) was dissolved in 80–90 mL of 2-propanol under vigorous stirring at ≃50 °C and subsequently diluted to a total volume of 920 mL. 80 mL of a 2×10^{-2} M NaOH solution in 2-propanol (pellets of sodium hydroxide dissolved in 2-propanol at ≃50 °C) was then added at 0 °C within 1 min under continuous stirring. The mixture was then immersed for 2 h into a water bath preheated to 65 °C. After 3 days of further aging at room temperature the solvent was removed by rotary evaporation (conditions: 30 °C, 1 Torr) of 10–50-mL aliquots of the isopropanolic ZnO colloid. The remaining hygroscopic white film was immediately resuspended in water to yield a transparent aqueous colloid (pH 7.7). Acetonitrile also dissolved the film yielding colloidal ZnO in an organic solvent.

A flow system consisting of a 250-mL thermostated reactor connected through short silicon and Tygon tubes with a Masterflex peristaltic pump (flow rate ca. 100 mL/min) and a flow cell (Hellma No. 176.50, light path 10 mm, height 11 mm, width 4 mm) was used for investigations of the time evolution of the absorption spectra. Mixtures of the zinc salt and the NaOH solutions in 2-propanol were prepared at the desired temperature and immediately introduced into the flow system. Spectra were recorded for 1 s at regular intervals with the HP 8451A diode array spectrophotometer and stored for further treatment. UV cutoff filters were used when appropriate.

Characterization of the Surface of the Colloidal Particles. Titrations of 40-mL samples of 1×10^{-3} M aqueous colloidal ZnO, thermostated to 25 °C, were carried out with a Radiometer autotitration system consisting of a pHM84 pH meter, a TTT80 titrator, and a ABU80 autoburet. A vigorously stirred suspension of ZnO colloid was titrated with freshly prepared 1×10^{-2} M stock solutions of NaOH (N_2 bubbled) or HCl at a rate of 10 μmol min^{-1}.

Coagulation studies were performed using the above-described flow system at 25 °C and monitoring the absorption changes in the visible (λ_{obsd} = 500 nm). The lack of any absorption of zinc oxide at this wavelength due to electronic transitions allows the observation of particle coagulation that results in an increase in light scattering of the solution (i.e., an increase of the apparent absorption due to forward scattering). In typical experiments, 40 mL of 1×10^{-3} M aqueous colloidal ZnO solutions was titrated at a rate of 5×10^{-7} mol min^{-1} starting at pH 7.6 with a 1×10^{-2} M solution of NaOH, while the absorbance was recorded. The first derivative of the absorption vs. time profile yielded the coagulation rate as a function of pH.

Results

The UV/vis absorption spectra recorded at various times during the preparation of a stable transparent suspension of ZnO colloid in 2-propanol are shown in Figure 1a. Thirteen seconds after mixing the zinc acetate with the base solution at 0 °C an onset of absorption (determined by the linear extrapolation of the steep part of the UV absorption toward the base line) λ_{os} = 306 nm is observed. The absence of any detectable particles in the electron

(35) Bahnemann, D.; Henglein, A.; Spanhel, L. *Faraday Discuss. Chem. Soc.* **1984**, *78*, 151.
(36) Weast, R. C., Astle, M. J., Beyer, W. H., Eds. *CRC Handbook of Chemistry and Physics*; CRC: Boca Raton, FL, 1985-86; Vol. 66, p D-92.
(37) Schindler, P.; Althaus, H.; Feitknecht, W. *Gazz. Chim. Ital.* **1963**, *93*, 168.
(38) Schindler, P.; Althaus, H.; Feitknecht, W. *Helv. Chim. Acta* **1964**, *47*, 982.
(39) Schindler, P.; Althaus, H.; Hofer, F.; Minder, W. *Helv. Chim. Acta* **1965**, *48*, 1204.
(40) Beutel, E.; Kutzelnigg, A. *Monatsh. Chem.* **1930**, *55*, 158.
(41) Bancroft, W. D.; Gurchot, C. *J. Phys. Chem.* **1932**, *36*, 2575.
(42) Nicoll, F. H. *J. Opt. Soc. Am.* **1948**, *38*, 817.
(43) Mollwo, E. *Z. Phys.* **1954**, *138*, 478.
(44) Hecht, H.; Mollwo, E. *Solid State Commun.* **1971**, *9*, 2167.
(45) Mollwo, E.; Zwingel, D. *J. Lumin.* **1976**, *12/13*, 441.
(46) Heiland, G.; Mollwo, E.; Stöckmann, F. *Solid State Physics*; Academic: London, 1959; Vol. 9, p 191.
(47) Riehl, N.; Ortmann, H. *Ber. Bunsen-Ges. Phys. Chem.* **1956**, *60*, 149.
(48) Dingle, R. *Phys. Rev. Lett.* **1969**, *23*, 579.
(49) Bhushan, S.; Pandey, A. N.; Kaza, B. R. *J. Lumin.* **1979**, *20*, 29.
(50) Takata, S.; Minami, T.; Nanto, H.; Kawamura, T. *Phys. Status Solids A* **1981**, *65*, K83.
(51) Minami, T.; Nanto, H.; Takata, S. *Thin Solid Films* **1983**, *109*, 379.
(52) Demas, J. N.; Crosby, G. A. *J. Phys. Chem.* **1971**, *75*, 991.
(53) Heller, H. G.; Langan, J. R. *J. Chem. Soc., Perkin Trans. 2* **1981**, 341.
(54) Skibfted, L. H.; Hancock, M. P.; Magde, D.; Sexton, D. A. *Inorg. Chem.*, submitted for publication.

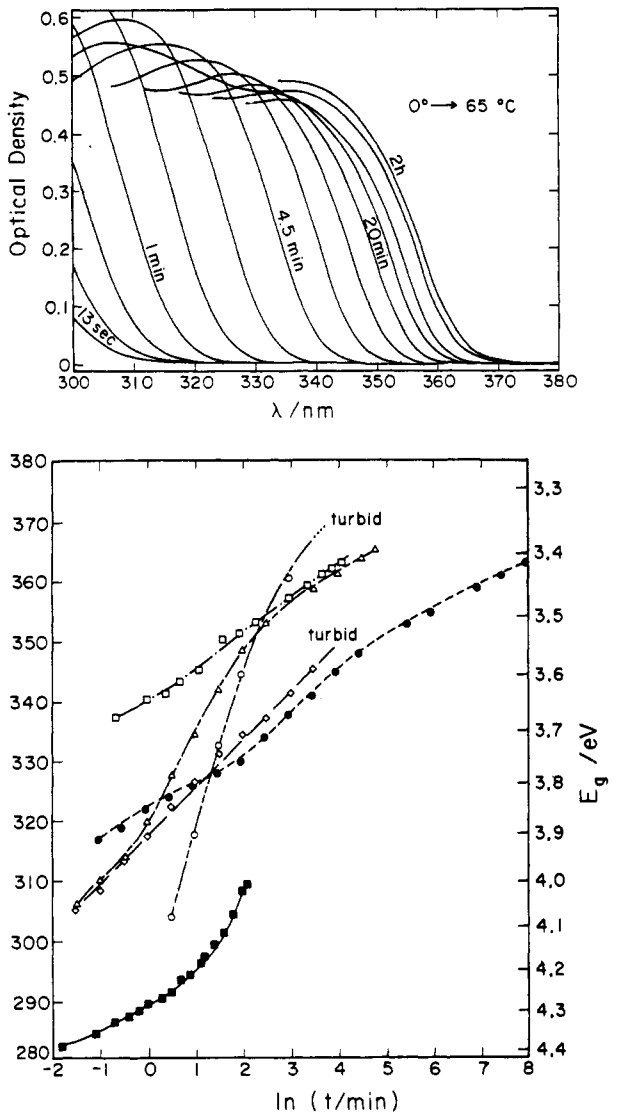

Figure 1. (a, upper) Absorption spectra taken at various times (logarithmic time scale) after mixing 1.0×10^{-3} M $Zn(OAc)_2$ with 1.6×10^{-3} M NaOH in 2-propanol at 0 °C for 1 min. Thereafter the solution is immersed into a preheated water bath at 65 °C. (b, lower) Onset of absorption as a function of time for various preparations of ZnO in 2-propanol: (□) 50 °C, (●) 25 °C, (■) 8 °C, with 3.3×10^{-3} M $Zn(OAc)_2$ and 3.3×10^{-3} M NaOH; (△) 0 °C → 65 °C, with 1.0×10^{-3} M $Zn(OAc)_2$ and 1.6×10^{-3} M NaOH; (◇) 25 °C, (○) −10 °C → 65 °C, with 1.0×10^{-3} M $Zn(ClO_4)_2$ and 1.6×10^{-3} M NaOH.

micrographs taken with a freshly prepared sample indicates that only extremely small ZnO particles are present at this stage (species with diameters $d \leq 5$ Å fall below the detection limit of the TEM). Upon continuous heating for 2 h at 65 °C λ_{os} steadily shifts toward 365 nm. Electron microscopy reveals that the reaction mixture now contains almost spherical particles with a mean diameter of 50 Å and a relatively narrow size distribution (±5 Å) as shown in Figure 2a. Plots of λ_{os} vs. the logarithm of the reaction time are given in Figure 1b for the results shown in Figure 1a as well as for various isothermal preparations. Data of analogous experiments using zinc perchlorate instead of zinc acetate are also presented in this diagram. Despite a rather similar dynamic behavior the formation of turbid suspensions is indicated with perchlorate as the anion; i.e., coagulation of the particles takes place. The linearity of this semilogarithmic presentation in the case of isothermal syntheses at 25 and 50 °C reveals that the spectral shift is strongly retarded toward the end of the preparation.

Some other features should be noted from the growth curves shown in Figure 1b:

The pronounced temperature dependence of the particle growth suggests that activation and not diffusion-controlled processes occur. A reaction mixture of acetate and base kept at 25 °C, for instance, needs 50 h to reach the same onset of absorption (363 nm) as an identical mixture at 50 °C after 1 h.

The choice of the anion is critical for the preparation of transparent, stable ZnO colloids. It has already been mentioned that the use of zinc perchlorate instead of zinc acetate yields a turbid suspension. λ_{os} initially changes more slowly in the case of zinc perchlorate. However, after a few minutes at 65 °C, when $\lambda_{os} = 360$ nm is reached, the colloid coagulates. A preparation made up of zinc acetate and base remains transparent for more than 2 h at 65 °C before precipitation. Experiments with $ZnCl_2$ or $Zn(NO_3)_2$ and otherwise similar reaction conditions reveal an even faster coagulation than in the case of $Zn(ClO_4)_2$ following the initial formation of a clear colloidal suspension.

A strong visible fluorescence is noted for all colloidal suspensions of ZnO. Figure 3 shows absorption and fluorescence spectra of isopropanolic suspensions of ZnO colloid at various growth stages. Excitation wavelengths for the fluorescence spectra were chosen to ensure identical absorbancies of the suspensions. As illustrated in Figure 3, the absorption spectra of freshly prepared colloidal suspensions of ZnO are characterized by blue-shifted onsets of absorption. Furthermore, pronounced absorption maxima ≈25 nm below λ_{os} are noted for the young preparations. Their fluorescence spectra (shown on the right-hand side of Figure 3) exhibit a single broad fluorescence band with an initial maximum around 460 nm. Concomitant to the changes of λ_{os} a bathochromic shift of this visible emission is perceived upon aging of the colloid. In fact the visible fluorescence appears to be consistently red-shifted by 155 ± 5 nm compared to λ_{os}. While the former peak changes from 460 to 516 nm, its intensity passes through a maximum with the highest fluorescence quantum yield of $\phi \approx 0.16$ measured for a sample that had been reacting at 25 °C for 2 min. After the colloidal suspension has been aged either by heat treatment or long reaction times (i.e., the ZnO colloids have reached their final growth stage as defined by a value of 365 nm for λ_{os}), a second fluorescence is encountered at 365 nm coinciding with the onset of the absorption spectrum. However, young ZnO colloids do not exhibit this fluorescence band.

Absorption and fluorescence spectra of an aqueous colloidal suspension containing 1×10^{-3} M zinc oxide at pH 7.7 are shown in Figure 4. The absence of absorption above 370 nm indicates that this suspension does not scatter light to any appreciable extent in the visible part of the spectrum. This is consistent with the observation (see TEM in Figure 2b) that particle sizes and size distribution have not changed during the preparation of the aqueous sample. However, upon comparison of parts a and b of Figure 2, the formation of chains of ZnO particles is obvious in the latter. Similar observations have been made before during the electron microscopy of aqueous TiO_2 colloids.[55] It is not yet clear whether these chains were already present in solution or were formed upon preparation of the samples for TEM. Recent investigations in this laboratory show the absence of comparable aggregation effects during the electron microscopy of aqueous α-Fe_2O_3 colloids.[56]

The onset of the absorption spectrum for the aqueous suspension, which is shown in Figure 4 is located also at 365 nm. Two maxima are again observed in the fluorescence spectrum, one coinciding with λ_{os} and a green emission at 520 nm. Fast titration to pH 12 likewise yields a transparent sol with similar spectral features.

The reflection and fluorescence spectra of zinc oxide powder (Baker, U.S.P.) are given in parts a and b of Figure 5, respectively. The white powder absorbs practically all UV light below 370 nm (i.e., with energies greater than 3.35 eV). Two fluorescence maxima are noted in the emission spectrum when the powder sample is irradiated with UV light ($\lambda_{ex} \leq 370$ nm). A first sharp fluorescence peak (fwhm ≈ 15 nm) appears at 380 nm, coinciding with the onset of the reflectance drop (Figure 5a). The second

(55) Spanhel, L. Diplomarbeit, Technische Universität Berlin, FRG, FB 6, 1985.
(56) Bahnemann, D. W.; Hoffmann, M. R., unpublished results.

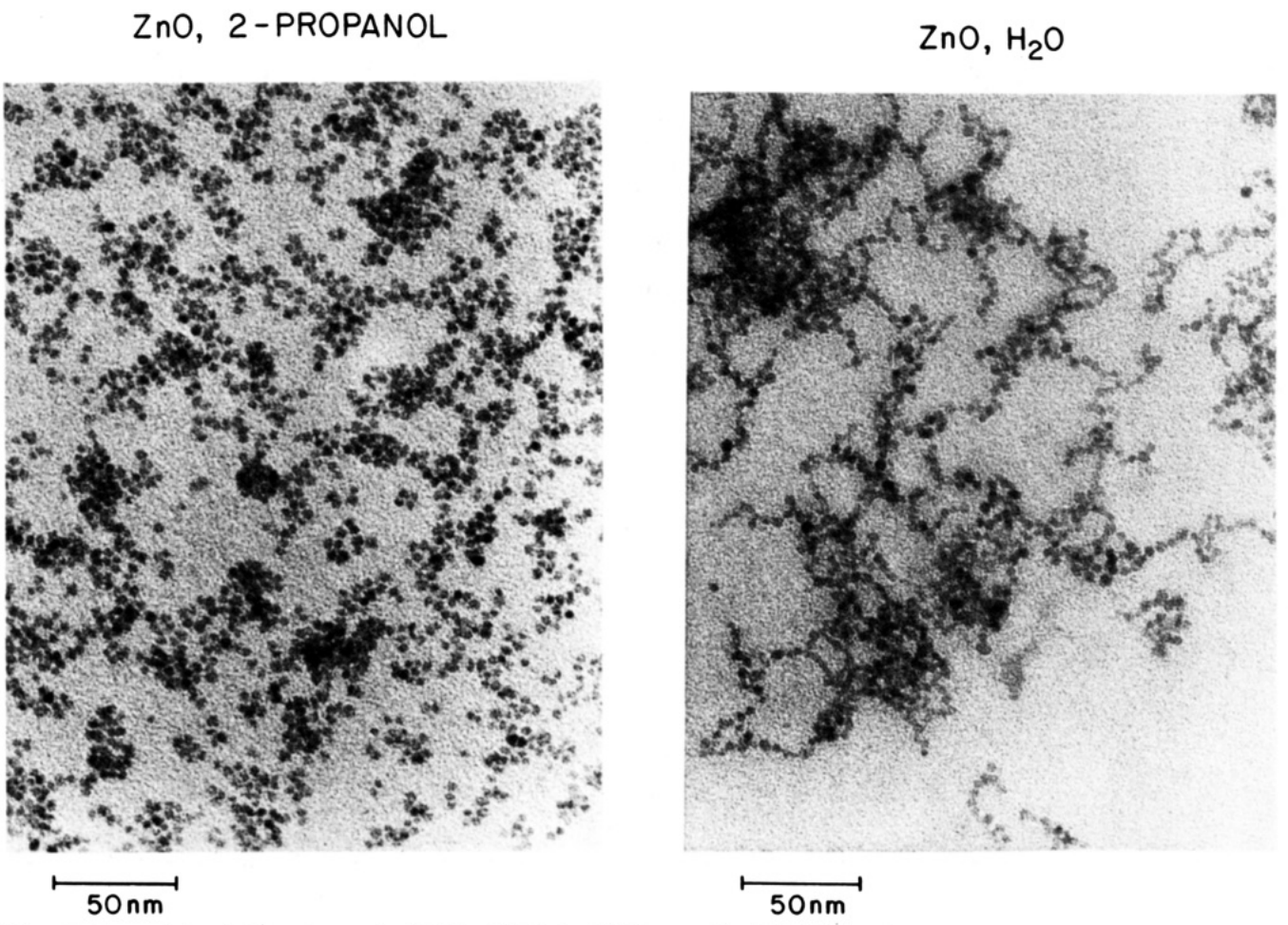

Figure 2. Transmission electron micrographs of ZnO colloid in (a, left) 2-propanol and (b, right) water.

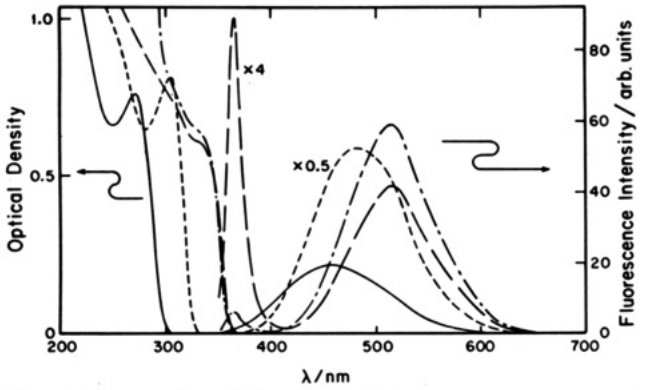

Figure 3. Superposition of absorption and fluorescence spectra measured in 2-propanol at various times after mixing 1.0×10^{-3} M $Zn(OAc)_2$ with 1.6×10^{-3} M NaOH: —, 30 s at 25 °C, after mixing at 0 °C (λ_{ex}^{n} = 280 nm); ---, 15 min at 25 °C (λ_{ex}^{n} = 310 nm); – – –, 2 h at 50 °C, 15 h at 25 °C (λ_{ex}^{n} = 340 nm); – – –, 2 h at 65 °C, 70 h at 25 °C (λ_{ex}^{n} = 340 nm).

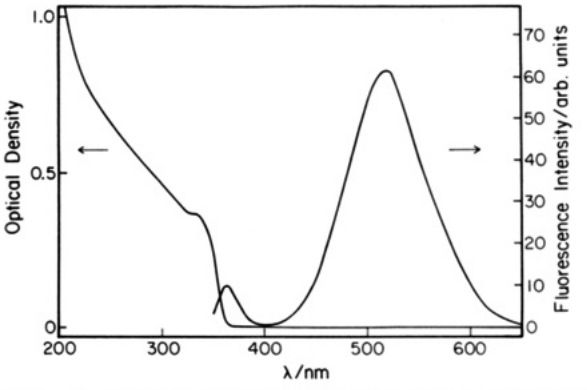

Figure 4. Absorption and fluorescence spectra of aqueous ZnO colloid (1×10^{-3} M ZnO, 2×10^{-3} M acetate, pH 7.7, air).

rather wide (fwhm ≈ 90 nm) green fluorescence band has its maximum around 510 nm.

Titration experiments have been conducted to determine the acid–base properties of colloidal ZnO. The initial pH of a 1×10^{-3} M aqueous suspension of ZnO colloid containing 2×10^{-3} M acetate (this anion is inherently present in all samples from their preparation) is 7.7 as shown in Figure 6. Titration with base promotes coagulation, while titration with acid leads to the dissolution of the colloid below pH 7.4. Figure 6 clearly shows that the pH increases upon addition of aqueous NaOH and eventually passes through an inflection point at pH 9.3 (after 45 μmol of base, i.e., 4.5 mL of a 1×10^{-2} M NaOH solution, have been added to 40 mL of 1×10^{-3} M ZnO). On the other hand, 100 μmol of HCl can be added with no pronounced change in pH, indicating a significant buffering capacity of the oxide system. Another inflection point is noted at pH 6.4. The slow drop of pH below pH 5.5 is well explained by the buffering capacity of the acetate.

Plots of the intensities of the UV (λ_{em} = 365 nm) and the green (λ_{em} = 516 or 520 nm) fluorescence as a function of the O_2 partial pressure are shown in parts a and b of Figure 7 for 3.3×10^{-4} M colloidal suspensions of ZnO in 2-propanol and water, respectively. While a similar qualitative behavior is observed in both cases, the fluorescence intensities of the isopropanolic are almost 1 order of magnitude larger than those of the aqueous colloid. Only 20% of this difference is due to the higher extinction coefficient of the isopropanolic sol at the excitation wavelength.

Both fluorescence peaks are initially present in carefully evacuated samples of ZnO. Upon exposure to the weak monochromatic light of the spectrofluorometer (λ_{ex} = 330 nm) a noticeable dynamic behavior is observed. The green emission is

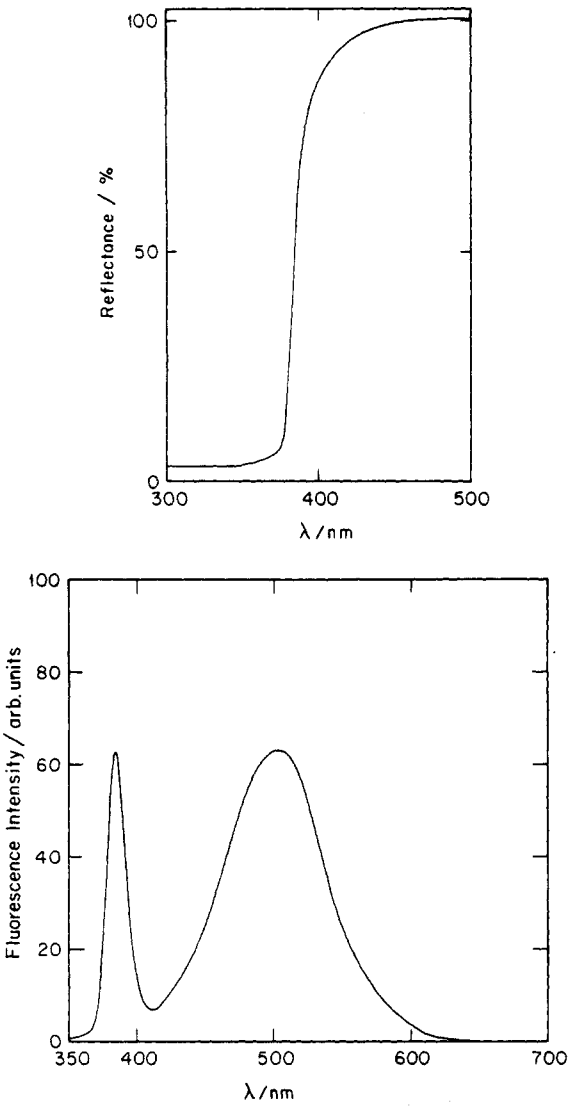

Figure 5. Powder spectra of ZnO crystals: (a, upper) reflectance and (b, lower) fluorescence, $\lambda_{ex} = 320$ nm.

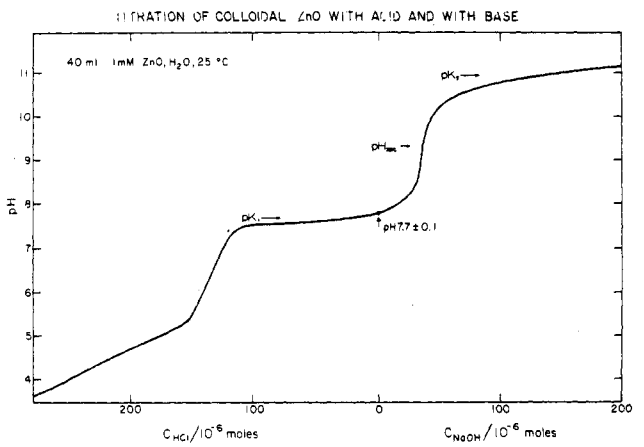

Figure 6. Titration curve obtained upon addition of 10^{-2} M HCl or 10^{-2} M NaOH to 40 mL of an aqueous ZnO colloid (1×10^{-3} M ZnO, 2×10^{-3} M acetate, 25 °C, air).

diminished by more than 1 order of magnitude within 5 s of illumination (≤ 10 μM photons have been absorbed by the sol during this period), while a considerable increase of the UV band occurs concurrently. No further changes of both fluorescence intensities are observed when the sol is exposed to the spectrofluorometer light for an additional period of 3 min (the time usually necessary to measure a complete emission spectrum). It should also be noted that the absorption spectrum of the colloidal

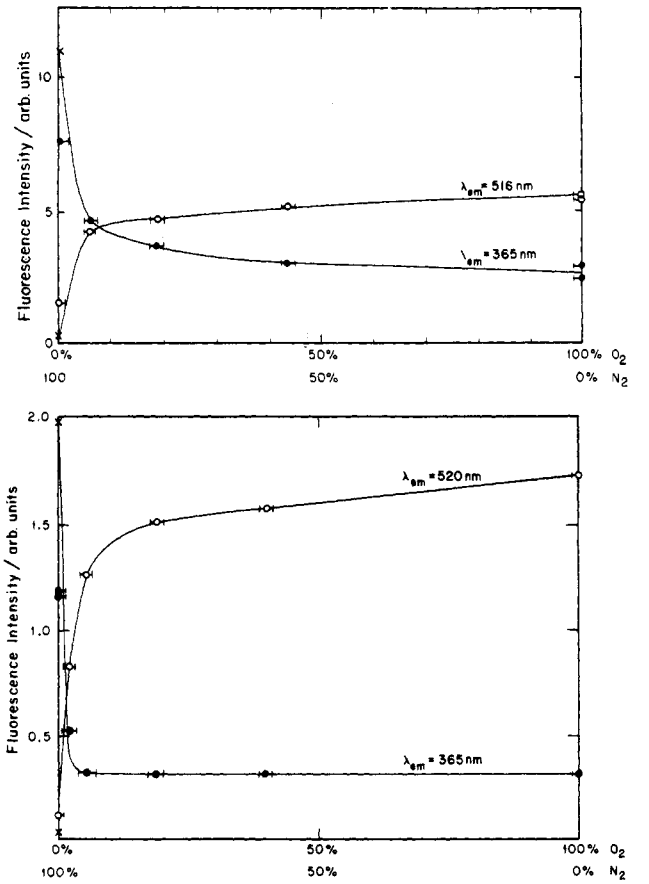

Figure 7. Fluorescence intensity (at equilibrium, see Results section) as a function of O_2 content: —O—/—●—, O_2/N_2 gas mixtures; ×, evacuated samples. (a, upper) 3.3×10^{-4} M ZnO in 2-propanol and (b, lower) 3.3×10^{-4} M ZnO in water.

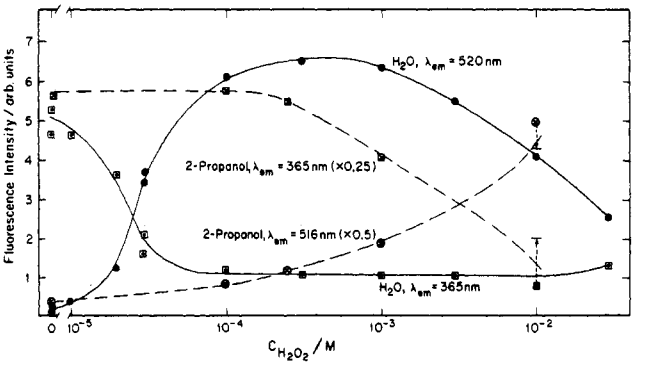

Figure 8. Fluorescence intensity as a function of the H_2O_2 concentration (3.3×10^{-4} M ZnO, evacuated samples).

suspension remained virtually unchanged during all the experiment described in Figures 7 and 8. Even though only an estimate of the initial magnitude of the two luminescence peaks can be given due to the instrument's limited time resolution ($\simeq 1$ s), we are confident that they do not differ by more than 20% from the values measured in aerated samples.

Following this short preirradiation period evacuated suspensions of ZnO fluoresce predominantly at 365 nm (cf. Figure 7, ×) with the intensity of this emission a factor of 3 or 7 higher than in oxygenated isopropanolic or aqueous colloids, respectively. All points given in Figure 7 represent equilibrium values measured subsequent to the initial dynamic behavior. Apparent differences between the results obtained for samples under vacuum and under N_2 can thus be explained by traces of O_2 still present in the nitrogen stream. The magnitude of the green fluorescence peak increases significantly with increasing content of molecular oxygen. In both suspensions, an O_2 concentration of 2.5% by volume is sufficient to promote 50% of the maximum intensity of the visible

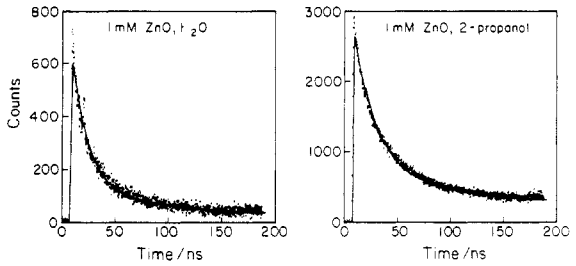

Figure 9. Fluorescence decay curves of ZnO colloid; solid lines represent a biexponential mathematical fit (see text).

emission, while at the same time the UV fluorescence intensity decreases (cf. Figure 7). In isopropanolic suspensions this decay closely matches the observed increase at λ_{em} = 516 nm. Air-saturated sols of ZnO in water exhibit a very weak UV emission but their 365-nm fluorescence in 2-propanol is more than 1 order of magnitude higher. Minor changes in the emission intensities are encountered between aerated and 100% oxygenated colloids of ZnO.

Addition of hydrogen peroxide also results in a green fluorescence and a lower UV emission as shown in Figure 8. However, a substantial difference in the response of the aqueous and the isopropanolic sols in the presence of H_2O_2 is apparent. In the former case, addition of 5×10^{-5} M H_2O_2 yields 50% of the maximum intensity of the visible and suppresses half of the initial UV emission. For H_2O_2 concentrations above 10^{-3} M the green fluorescence is depressed. In the case of the isopropanolic colloids, higher concentrations of H_2O_2 (100-fold) are required to suppress 50% of the UV fluorescence, whereas the green emission increases slightly without reaching a limiting value.

Figure 9 shows the time-resolved decay curves of the visible emission of colloidal suspensions of ZnO where the solid lines represent a double-exponential decay according to the following formula:

$$I(t) = I_1(0)e^{-t/\tau_1} + I_2(0)e^{-t/\tau_2}$$

This fit accounts for the fate of ≃90% of the observed emission. For a 10^{-3} M suspension of ZnO colloid in 2-propanol, 80% of the intensity decays with a characteristic time (τ) of 17 ns, while the remainder decays with τ = 190 ns. The aqueous suspension shows that 84% of the intensity decays with a characteristic time of 14 ns and the remainder with τ = 140 ns. The data for the decay of the UV emission suggest, on the other hand, that its lifetime is less than 100 ps and probably even less than 50 ps (rise time of the photomultipier employed in this study) in both sols. Experiments with a higher time resolution are thus required to resolve differences between the two colloidal preparations.

Table I summarizes rate constants obtained from the Stern–Volmer analysis of fluorescence quenching studies at λ_{em} = 520 nm using aqueous colloidal suspensions of ZnO. Plotting ϕ_0/ϕ vs. the concentration of the quencher (Q) yields straight lines with slopes denoted conventionally as $k_q\tau$ (see second column of Table I):

$$\phi_0/\phi = 1 + k_q\tau[Q]$$

Taking a lifetime τ of the visible fluorescent center of 14 ns, as obtained by the kinetic decay measurements, the bimolecular quenching constant k_q can be calculated (third column). Values between 10^{13} and 10^{15} M^{-1} s^{-1} indicate that at pH 7.7 oxidizing molecules like MnO_4^- or $Cr_2O_7^{2-}$ but also nonoxidizing cations, e.g., Fe^{2+}, are extremely efficient quenchers. Other cations such as Ni^{2+} or Co^{2+} also quench the green fluorescence yielding straight Stern–Volmer plots with lower bimolecular rate constants. Methylviologen (1,1′-dimethyl-4,4′-bipyridinium chloride, MV^{2+}) and Ag^+ are inefficient quenchers at pH 7.7. At pH 12, quenchers which are ineffective at pH 7.7 such as MV^{2+} and Ag^+ are more efficient by a factor of about 10^2. Anions such as $Cr_2O_7^{2-}$ and MnO_4^- which are most effective at pH 7.7 are less effective at pH 12.

TABLE I: Quenching of the Visible Emission of Aqueous ZnO Sols

quencher	$k_q\tau/M^{-1}$	k_q[a]$/M^{-1}$ s^{-1}
	At pH 7.7	
MnO_4^-	8×10^6	6×10^{14}
$Cr_2O_7^{2-}$	3×10^6	2×10^{14}
Fe^{2+}	2.0×10^6	1.4×10^{14}
Cu^{2+}	6.4×10^5	4.6×10^{13}
Fe^{3+}	3.5×10^5	2.5×10^{13}
Cr^{3+}	1.6×10^5	1.1×10^{13}
Zn^{2+}	1.6×10^4	1.1×10^{12}
Co^{2+}	5.9×10^3	4.2×10^{11}
Ni^{2+}	1.7×10^3	1.2×10^{11}
Mn^{2+}	1×10^3	7×10^{10}
MV^{2+}	$\approx 8 \times 10^2$	$\approx 6 \times 10^{10}$
Ag^+	$\approx 5 \times 10^2$	$\approx 4 \times 10^{10}$
	At pH 12	
MnO_4^-	3.7×10^5	2.6×10^{13}
Ag^+	3×10^5	2×10^{13}
MV^{2+}	1.2×10^5	8.6×10^{12}
Mn^{2+}	3.7×10^4	2.6×10^{12}
Co^{2+}	3.2×10^4	2.3×10^{12}
$Cr_2O_7^{2-}$	7×10^3	5×10^{11}
Li^+	$<10^2$	$<7 \times 10^9$

[a] Assuming $\tau = 14 \times 10^{-9}$ s from the fluorescence decay time measurement.

When permanganate or dichromate is used as quencher a time-dependent relationship is noted. For example, 1×10^{-6} M MnO_4^- is sufficient to reduce the emission intensity at 520 nm by a factor of 9 (1×10^{-3} M ZnO, pH 7.7, air, λ_{ex} = 330 nm). Continuous illumination with a weak light source (e.g., 8×10^{-8} M photons absorbed per second by the colloidal suspensions) results in a subsequent increase of the fluorescence intensity over a period of 1 min until it reaches about 75% of the intensity value it had without adsorbates. Similar phenomena are observed at pH 12 or when $Cr_2O_7^{2-}$ is employed instead of MnO_4^-. All values reported in Table I refer to the initial emission intensities.

The optical properties of an evacuated sample of ZnO colloid are changed upon prolonged ultrabandgap illumination as shown in Figure 10. The absorption and fluorescence spectra of an aerated solution of 1×10^{-3} M ZnO in 2-propanol containing 2×10^{-3} M acetate and 6×10^{-6} M methylviologen are given as a reference (full line). The absorption spectrum of an evacuated solution which has been irradiated with 60 μM photons (λ_{ex} = 330 nm) shows the characteristic pattern of reduced methylviologen, $MV^{\bullet+}$,[57] at 396 nm. However, no change is noted in the UV portion of the absorption spectrum which is characteristic for ZnO. Concurrently, the UV emission increases in intensity while the green fluorescence decreases by about 1 order of magnitude. This effect has already been described when the O_2 dependence of the fluorescence was studied (Figure 7a). Further irradiation with 10 mM photons results in a shift in the absorption spectrum of λ_{os} from 365 to 345 nm. In addition, the blue color of $MV^{\bullet+}$ disappears. The new absorption pattern near 396 nm is characteristic of doubly reduced methylviologen, MV^0.[57] The fluorescence spectrum of this extensively irradiated solution features only the UV emission redshifted to 368 nm. When the colloidal suspension is exposed to air the blue color of $MV^{\bullet+}$ reappears. After 30 s of exposure, the absorption and fluorescence spectra return to the original reference spectra with slight variations in the intensities.

Discussion

Synthesis. The results clearly show that we have been able to synthesize stable transparent solutions of colloidal ZnO suspended in either water, 2-propanol, or acetonitrile. Since the formation of zinc oxide in water is not favorable compared to the formation of $Zn(OH)_2$[36-39] (vide supra) synthesis in a nonaqueous solvent was found to be necessary. Zinc acetate in the presence of 80% of the stoichiometric amount of NaOH yields the most stable

(57) Watanabe, T.; Honda, K. *J. Phys. Chem.* **1982**, *86*, 2617.

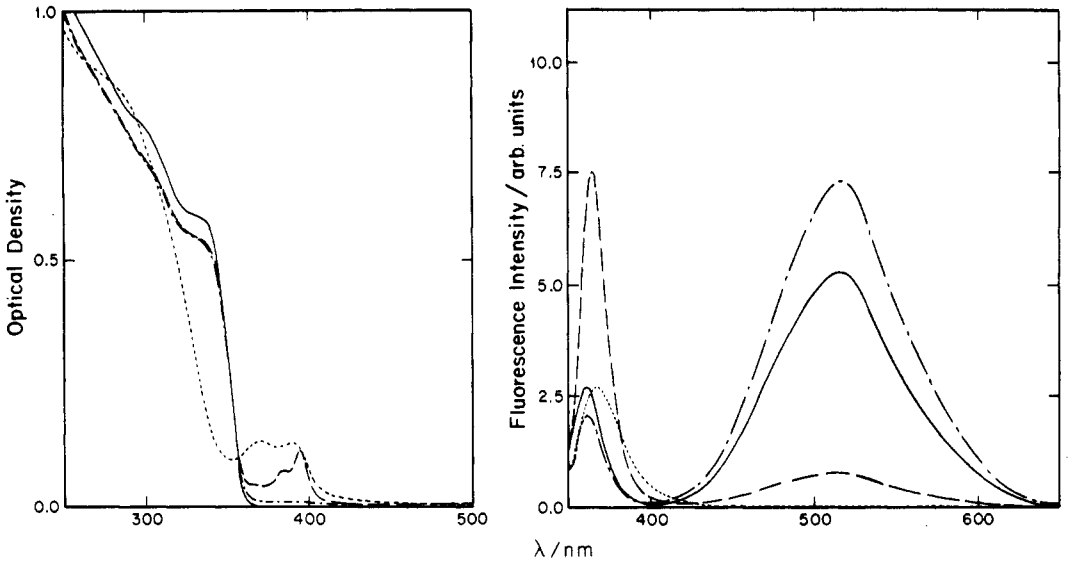

Figure 10. Effect of illumination on the spectroscopic properties of colloidal ZnO, 1×10^{-3} M ZnO, 2×10^{-3} M acetate, 6×10^{-6} M methylviologen, in 2-propanol, $\lambda_{ex} = 330$ nm; —, aerated, no $h\nu$; – –, evacuated, 6×10^{-5} M $h\nu_{abs}$; - - -, evacuated, 1×10^{-2} M $h\nu_{abs}$; – · –, evacuated, 1×10^{-2} M $h\nu_{abs}$, 30 s air.

colloids when 2-propanol is the solvent. Comparison of the spectroscopic properties of ZnO powder (Figure 5) with those of the colloidal preparations in 2-propanol (Figure 3) or water (Figure 4) reveals that this synthesis resulted in the desired product. The formation of zinc hydroxide, which would not result in spectral changes above 220 nm, is not indicated. Moreover, the X-ray diffraction patterns of crystalline ZnO and a powder prepared from the sol qualitatively show similar features, but the quantitative comparison reveals the presence of amorphous material in the colloidal preparation. Even though colloid stabilizers were intentionally not used in this study, the pronounced dependence of the kinetics of synthesis on the type of anion (Figure 1b) and the subsequent stabilization of the final suspension suggests that acetate does stabilize the sol. However, the nature of this effect is not consistent with simple double layer theory in that the acetate anion should destabilize the positively charged ZnO surface. It is also unlikely that the stabilizing activity of a small molecule like acetate could stem from a steric hindrance of the coagulation that occurs with some polymeric stabilizers.

UV/Vis Spectra. During the course of the synthesis of ZnO suspensions in 2-propanol significant spectroscopic changes were observed (Figures 1 and 3); similar observations have been made by others during the preparation of ultrasmall particles of ZnS, CdS, PbS, Zn_3P_2, Cd_3P_2, Cd_3As_2, CuCl, AgCl, AgBr, AgI, and PbI_2.[7-28] These changes have been explained by the "quantum (Q)-size effect" and can be attributed to the gradual transition from ZnO clusters, $(ZnO)_n$ with n starting perhaps as low as 8 or 16[16] to $(ZnO)_n$ particles with $n \approx 3000$ (assuming spherical geometry of the colloidal particles this value of n was estimated from the mean diameter as observed by TEM (Figure 2)). The latter particles exhibit photophysical and photochemical[58] properties of the bulk semiconductor material. Quantum mechanical calculations have been described by Brus[4-6] to account for these shifts of the electronic levels in the Q-state. For a sphere with a radius R and a dielectric coefficient ϵ he derived the following formula to calculate the energy E^* of the lowest excited state of the exciton

$$E^* \simeq E_g + 0.5\hbar^2\pi^2R^{-2}(m_e^{-1} + m_h^{-1}) - 1.8e^2\epsilon^{-1}R^{-1}$$

where E_g is the bulk bandgap energy and m_e and m_h are the effective masses of the electron and hole, respectively. This equation predicts that the energy level of the first excited state increases as the cluster size (R) decreases. Henglein and coworkers, on the other hand, have used a semiclassical treatment[16] and subsequently various quantum-mechanical approaches[22,59] to predict the dependence of the onset of absorption upon particle size. They observed good qualitative agreement with experimental data in the case of CdS.[22]

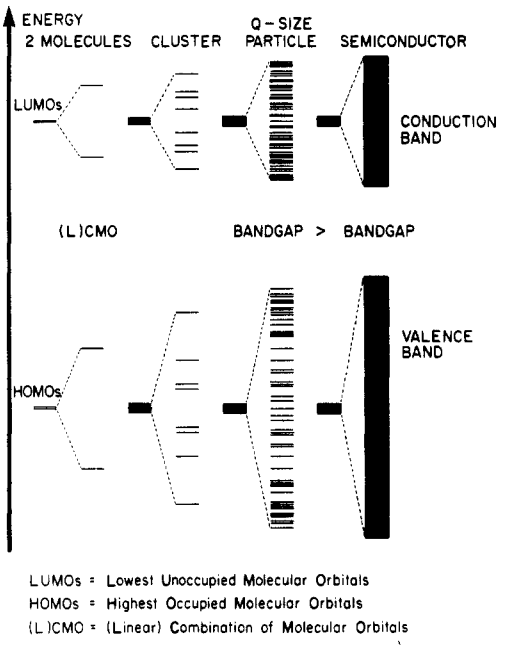

Figure 11. MO model for the particle growth.

Throughout the following discussion we shall use an alternative qualitative molecular orbital (MO) picture[60] to account for the bathochromic spectroscopic shift observed during the early growth stages of ZnO (Figure 11). It is obvious from this figure how the splitting of energetic levels into a filled and an empty region proceeds as the number of contributing MO's increases. In large particles the ensemble of energetic levels becomes dense yielding the valence and the conduction band, respectively. Since electronic transitions from the highest occupied molecular orbitals (HOMO's) to the lowest unoccupied molecular orbitals (LUMO's) yield the observed absorption spectrum the blue-shifted λ_{os} is readily explained for the Q-size particles.

It is interesting to note that ZnO particles must be smaller than 50 Å before a bandgap shift becomes obvious. In a recent in-

(58) Kormann, C.; Bahnemann, D. W.; Hoffmann, M. R., to be published.

(59) Schmidt, H. M.; Weller, H. *Chem. Phys. Lett.* **1986**, *129*, 615.

(60) Atkins, P. W. *Physical Chemistry*; Oxford University Press: Oxford, U.K., 1978; p 484.

vestigation Spanhel[55] showed that TiO_2 crystallites of only 36 Å diameter still show the same λ_{os} as the bulk material. On the other hand, CdS particles exhibit Q-size effects until particle sizes with diameters around 80 Å are reached.[22] Properties of the respective anions such as size and polarizability seem to be important factors determining the quantum size regime of a material.

Transition probabilities between the MO's are also governed by symmetry selection rules, which become more important as the total number of orbitals decreases. This might explain the pronounced maximum structure observed in the absorption spectra of very small ZnO clusters, indicating that transitions of narrow energy distribution and high probability occur (cf. Figure 3).

Surface Properties. A more detailed description of the surface structure of metal oxides is useful for the better understanding of surface phenomena and for the discussion of the fluorescence behavior of our colloidal particles. In water, metal oxide surface chemistry is controlled by surface hydroxyl groups.[61] The following equilibria must be considered:

$$\equiv MOH_2^+ \rightleftharpoons \equiv MOH + H^+ \qquad pK_1 \qquad (2)$$

$$\equiv MOH \rightleftharpoons \equiv MO^- + H^+ \qquad pK_2 \qquad (3)$$

In some cases pK_1 and pK_2 values may be determined by titration.[61] The surface chemical properties of an oxide surface are sensitive to the composition of the aqueous phase because specific adsorption or binding of solutes to the surface can occur. The surface charge together with the pH of zero point of charge ($pH_{zpc} = {}^1/_2(pK_1 + pK_2)$) are important properties of oxide particles. Besides the above-mentioned charges due to ionizable hydroxo groups, lattice imperfections and the adsorption of surfactant ions are responsible for surface charges. Titration studies as well as experiments aimed at determining the rate of coagulation of the colloidal particles allow the determination of pH_{zpc}.

The acid titration of aqueous colloidal ZnO (Figure 6) results in an estimated value for pK_1 of 7.6 ± 0.1 (flat part of the curve, reflecting the buffering capacity of the surface with similar concentrations of protonated and neutral surface groups). Under the assumption that the surface charge is due only to ionized hydroxo groups (equilibria 2 and 3) a pH_{zpc} of 9.3 ± 0.2 can be derived from the inflection point in Figure 6. Since specific adsorption of carbonate or acetate could have lowered the pH_{zpc}—in fact, specific adsorption of impurities such as fatty acids can provoke a shift in the pH_{zpc} of more than two pH units[62]—additional titration–coagulation experiments were performed. The coagulation rate (as determined by the rate of the sol's turbidity increase) is expected to be a maximum at the pH_{zpc} due to surface electroneutrality. Titration studies with our aqueous ZnO sols showed that starting at pH 7.6 and titrating toward pH 11 the coagulation rate peaked at pH 9.2. These results for pH_{zpc} can be favorably compared with literature values for macrocrystalline ZnO that give a mean pH_{zpc} of 9.0 ± 0.3.[62]

Fluorescence Spectra. The luminescence maximum at 365 nm which closely coincides with the onset of absorption can be assigned as "bandgap" fluorescence caused by a transition from the lower edge of the conduction to the upper edge of the valence band. Temperature studies with bulk crystals are consistent with this interpretation.[44] The name "exciton" emission has been alternatively used[16,21] to describe the UV band of the luminescence spectrum in terms of a quantum-mechanical picture. Similar to earlier observations for CdS[16] small $(ZnO)_n$ clusters prepared in the presence of air do not exhibit this UV fluorescence, but particle growth to a size range $2000 \leq n \leq 3000$ is required for its occurrence (cf. Figure 3). Thus the lifetimes of electrons and holes in the conduction and valence band seem to increase with increasing particle size. However, for smaller clusters (i.e., $n \ll 3000$) relaxation into more favorable energy levels may result in an emission at longer wavelengths. This scheme is consistent with the observation that the yield of the visible emission goes through a maximum during the early stages of growth.

The nature of the visible fluorescence is more difficult to assign.[40-51] The concept of anion vacancies has been discussed by Henglein and co-workers for various n-type semiconductor materials.[15-21] They describe the fluorescence centers as a cation-rich structure ("anion vacancies") on the surface of a crystallite which can attract photogenerated electrons from the conduction band of particles such as ZnS[15] and ZnO.[21] The electronically excited crystallites can vibrationally relax to states of lower energy, which are geometrically different from the ground state. This interpretation explains why these levels are not accessible from the ground state, i.e., do not appear in the absorption spectrum (Franck–Condon principle), and why a radiative transition toward the ground state or to a trapped hole is characterized by a long lifetime. However, our findings are not consistent with this theory. While Koch et al.[21] observed that surface-bound excess zinc ions (i.e., anion vacancies) increased the 540-nm emission of their colloidal ZnO preparations in 2-propanol at pH 12, addition of Zn^{2+} to an aqueous colloid at pH 7.7 quenches this fluorescence in our system (see Table I). Moreover, alkaline colloids at pH 10.4, which should be characterized by cation vacancies due to a negatively charged surface, have almost the same fluorescence intensity as positively charged sols at pH 7.7.

Therefore, we envisage the physical nature of the fluorescence centers in ZnO to be like that proposed by Chestnoy et al.[14] In their study of the luminescence behavior of small CdS particles (22–38 Å in diameter) they attribute the visible fluorescence to photogenerated, trapped electrons tunneling to preexisting, trapped holes. Their model differs from the one previously proposed in that it does not require the presence of surface anion vacancies as a prerequisite for the occurrence of emissions with energies lower than the bandgap energy of the semiconductor. Multiexponential decay kinetics of the visible emission (cf. Figure 9) have also been observed by these authors who explained these results by a high probability of radiationless relaxation.[14]

As shown in Figure 7, the presence of molecular oxygen is essential for conversion of the UV emission into the visible fluorescence band. In an oxygen-free environment, relatively high concentrations of methylviologen (i.e., 10^{-4} M), which has a redox potential similar to O_2,[57] also enhance the 520-nm emission relative to the 365-nm band. Koch et al. recently reported similar observations when they described the disappearance of the visible emission of an evacuated aqueous suspension of colloidal zinc oxide upon UV irradiation.[21] A concurrent blue shift of the absorption spectrum of their sample was originally attributed to a physical shrinkage of the particles[21] but has since been reinterpreted in terms of excess electrons on the colloidal particles, influencing the energy of the exciton state.[23] Both effects were reversible in the presence of O_2. In their discussion, these authors explained the observed quenching of the visible fluorescence by the presence of excess electrons[23] or Zn^+ centers[21] reacting with photogenerated holes. The role of molecular oxygen was then proposed to be that of an e^- acceptor which restores the original conditions. Even though great similarities seem to exist between those results and our findings, substantial differences need to be pointed out:

No shift in the absorption spectra is observed in our ZnO sols while the fluorescence changes occur, suggesting that the presence of excess electrons and/or Zn^+ centers on the particles should be minimal. Several millimoles of photons are in fact necessary to provoke such spectral shifts (cf. later part of Discussion and Figure 10).

The intensity of the UV emission increases by a factor of 3 or 7 in the absence of molecular oxygen with 2-propanol or water being the solvent, respectively. This observation cannot be explained by the proposed mechanism which would most probably invoke the quenching of both fluorescence bands by the excess e^- but should at least not result in an increase of the UV emission.

While a possible explanation for the influence of molecular oxygen and methylviologen on the relative fluorescence intensities could be their electron-accepting ability, this simple picture cannot be applied to explain the marked differences in sensitivity toward H_2O_2 which are observed when either water or 2-propanol is the

(61) Stumm, W.; Morgan, J. J. *Aquatic Chemistry*, 2nd ed.; Wiley-Interscience: New York, 1981.
(62) Parks, G. A. *Chem. Rev.* **1965**, *65*, 177.

solvent (cf. Figure 8). A polar molecule such as hydrogen peroxide should rather be more strongly adsorbed to the hydrophilic ZnO surface in 2-propanol (dielectric constant $\epsilon_{25°C} = 18.3$) than in H_2O ($\epsilon_{25°C} = 78.5$) where it nevertheless exhibits a much higher activity in promoting the visible fluorescence.

In the following we propose a mechanism to explain our observations. The main pathway of energy dissipation is a radiationless relaxation as deduced from the overall low fluorescence yield for fully developed ZnO colloids ($\phi = 0.03$). In the absence of electron acceptors, part of the photogenerated conduction band electrons (e_{CB}^-) can also radiatively combine with valence band holes (h_{VB}^+) giving rise to the bandgap fluorescence. However, following the careful evacuation of our samples both fluorescence bands are initially still apparent with their relative intensities being similar to those observed in the presence of air. Absorption of a few micromoles of photons ($\lambda_{ex} \leq 365$ nm) results in the effective bleaching of the visible emission while there is a significant simultaneous increase of the UV emission (cf. Figure 7, ×). This observation can be explained by a photodesorption of trace amounts of molecular oxygen (reaction 4). O_2 is known to be

$$ZnO/O_2^{\bullet-} + e_{CB}^- + 2H_{aq}^+ \rightarrow ZnO + H_2O_2 \quad (4)$$

strongly chemisorbed to the surface of zinc oxide (probably in the form of superoxide, $O_2^{\bullet-}$, since an electronegative molecule such as O_2 readily accepts an excess electron from ZnO which is a typical n-type semiconductor) and thus cannot be removed under reduced pressure at room temperature.[63] The concentrations of hydrogen peroxide resulting from this reaction are too small (≤ 1 μM assuming the adsorption of one molecule of O_2 per ZnO particle) to have a noticeable influence on the fluorescence yields (cf. Figure 8).

The significant influence of adsorbed molecular oxygen and methylviologen can then be explained by a relay action of these compounds resulting in the formation of the respective radical ions via reactions 5 and 6. The intermediacy of these semireduced

$$e_{CB}^- + O_2(ads) \rightarrow O_2^{\bullet-}(ads) \quad (5a)$$

$$e_{CB}^- + MV^{2+}(ads) \rightarrow MV^{\bullet+}(ads) \quad (5b)$$

$$O_2^{\bullet-}(ads) + Tr \rightarrow Tr^- + O_2(ads) \quad (6a)$$

$$MV^{\bullet-}(ads) + Tr \rightarrow Tr^- + MV^{2+}(ads) \quad (6b)$$

species seems necessary for the conduction band electrons to find their way to the appropriate electron traps (Tr). The visible fluorescence then results from the tunneling of these trapped electrons to preexisting, trapped holes.[14]

The influence of hydrogen peroxide on the 520-nm emission band (cf. Figure 8) cannot be understood by a simple electron transfer in accordance with reactions 5 and 6 since the one-electron reduction of H_2O_2 is an irreversible process leading to the formation of hydroxyl radicals. It is therefore suggested that the valence band holes react with H_2O_2 via the overall reaction

$$2h_{VB}^+ + H_2O_2 \rightarrow O_2 + 2H_{aq}^+ \quad (7)$$

resulting in the generation of molecular oxygen which in turn acts as an electron relay (reactions 5a and 6a). The different sensitivity of the aqueous and the isopropanolic colloid toward hydrogen peroxide (cf. Figure 8) is then explained by a competition of the solvent for the photogenerated holes. 2-Propanol can act as a reductant and is thus able to accept h_{VB}^+; therefore a much higher H_2O_2 concentration is required to intercept the bandgap fluorescence than in the case of water as solvent. The decreasing effect of high concentrations (i.e., $>10^{-3}$ M) of hydrogen peroxide upon the intensity of the visible emission of ZnO in water is a quenching action which will be discussed in detail below. While the $O_2^{\bullet-}/O_2$ and the $MV^{\bullet+}/MV^{2+}$ redox couples serve as electron relays, the fluorescent center must be an *intrinsic* entity of the crystal because the nature of the electron relay does not affect the energy of the long-lived emission.

The fact that small ZnO clusters exhibit a much higher intensity of the green fluorescence than larger zinc oxide particles can be explained by the high specific surface area of the former leading to shorter distances to a surface-bound electron acceptor (e.g., O_2). In addition, due to a smaller number of crystal molecules, the phonon state density responsible for radiationless relaxation should be lower; i.e., there will be less channels for radiationless recombination.

Additional proof for the proposed electron-shuttle mechanism comes from results of an anoxic synthesis of ZnO in 2-propanol. Fluorescence measurements during the course of this synthesis revealed the occurrence of a UV emission at the early stages of the particle growth (i.e., where the solution contained only clusters consisting of a few zinc oxide molecules which are not detectable by TEM) matching the respective onset of the absorption spectrum. A bandgap fluorescence around 320 nm has, for example, been measured 1 min after mixing $Zn(OAc)_2$ with NaOH at 0 °C in a N_2-flushed glovebox in excellent agreement with the absorption onset observed at the same time (cf. Figure 1a). This luminescence subsequently shifted to longer wavelengths as the aging process occurred. The concurrent observation of a very small visible luminescence is explained by traces of O_2 still present in the reaction mixture. Upon exposure to air the UV emission immediately disappeared giving rise to the broad visible fluorescence that had been observed during the original preparations (cf. Figure 3). These results clearly support the proposed electron relay mechanism. This is, to the best of our knowledge, the first time that a blue-shifted bandgap fluorescence has been observed at these very early growth stages during the preparation of Q-size particles. Fojtik et al. also observed a UV emission shifted to shorter wavelengths as compared with the absorption onset of bulk crystals when they prepared small CdS particles.[16] However, this band only appeared with an onset of the concurrent absorption spectrum of $\lambda_{os} \geq 430$ nm; i.e., particle diameters above 25 Å had been reached.[22] While this value corresponds to almost 200 molecules of CdS per particle, an upper limit of $d = 10$ Å (estimated from the absence of any image in the TEM) suggests that each zinc oxide cluster contains only about 20 ZnO molecules as the UV fluorescence is observed.

Many of the bimolecular fluorescence quenching constants k_q (listed in Table I) exceed the limit of diffusion-controlled reactions. We conclude that the quenching molecules are adsorbed onto the surface of the colloidal particles at the moment of excitation. This is clearly indicated by the different behavior noted at pH 7.7 and pH 12. At pH 7.7 the cations Ag^+, Mn^{2+}, and MV^{2+} are poor quenchers (i.e., the ZnO surface is positively charged) whereas at pH 12 very steep Stern–Volmer plots are obtained. Anions such as MnO_4^- and $Cr_2O_7^{2-}$ are not accommodated readily on negatively charged surfaces but exhibit the highest quenching constants when positive sites are available at pH 7.7. We have in fact used this behavior as a third alternative to estimate the pH_{zpc} of our aqueous colloids by performing titrations in the presence of minute amounts of the appropriate quenchers and measuring the variations in the emission intensity at 520 nm. This method yields pH_{zpc} values in agreement with the results presented above. Some cations are very efficient quenchers even at pH 7.7, e.g., Cr^{3+}, Cu^{2+}, Fe^{3+}, and Fe^{2+}, suggesting that the electrostatic interaction is not the only force governing surface adsorption. We propose an electron-transfer mechanism to account for the fluorescence quenching. Strongly oxidizing adsorbates such as MnO_4^-, $Cr_2O_7^{2-}$, Fe^{3+}, and Ag^+ irreversibly accept photogenerated electrons without back donation to electron traps, whereas Fe^{2+} appears to act as a hole scavenger.

A limited number of quenching experiments have also been performed with 2-propanol as the solvent resulting in k_q values for the suppression of the visible emission similar to those given in Table I for the aqueous sol. However, since an aerated isopropanolic suspension of ZnO still exhibits a considerable bandgap fluorescence (cf. Figure 7a) its quenching was also studied. We noted a complete quenching of the UV emission with $k_q \geq 4 \times 10^{15}$ M^{-1} s^{-1} (e.g., Cu^{2+}) before the visible fluorescence appeared

(63) Many, A. *CRC Critical Reviews in Solid State Sciences*; CRC: Boca Raton, FL, 1974; p 515.

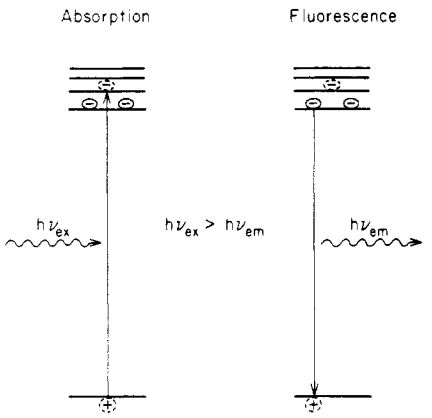

Figure 12. Spectroscopic properties of preirradiated ZnO.

to be affected. This observation is in good agreement with the above mechanism where an electron transfer from the conduction band should be more efficient than from a lower energy trap.

The dynamic behavior that has been observed when compounds such as MnO_4^- or $Cr_2O_7^{2-}$ were employed as fluorescence quenchers is explained by an efficient conversion of a strong oxidant, i.e., a good quencher, to a less effective species following the irreversible uptake of electrons.

Reversible Spectral Shifts. As shown in Figure 10 the absorption spectrum of an oxygen-free isopropanolic suspension of the colloidal particles can be shifted by 20 nm toward shorter wavelengths upon prolonged illumination ($\simeq$10 mM $h\nu$ with λ_{ex} = 330 nm were absorbed during the experiment). This spectral change which corresponds to a shift of 190 mV in the bandgap energy is found to be reversible once molecular oxygen is added to the system. Similar effects have been reported by Albery et al.[64] and Henglein and co-workers[23] for small CdS particles using flash and pulse radiolysis techniques, respectively. The latter attributed their observations to nonlinear optical effects and suggested that electrooptical applications of this phenomenon are indicated. A blue shift of the absorption spectrum that was observed by Koch et al. when they illuminated colloidal ZnO in the absence of oxygen was originally explained on the basis of a decrease in the size of the small ZnO particles[21] but subsequently also interpreted as a nonlinear effect.[23] These authors suggested that the presence of a single excess electron on a small semiconductor particle suffices to create a polarizing field which increases the energy of the excitonic state thus leading to a blue-shifted absorption spectrum.

However, our observations cannot readily be explained by this electrostatic model. While it describes the pronounced UV shift in the absorption spectrum very well, this theory is unable to account for the finding that the bandgap emission of the illuminated solution is *not* blue-shifted but rather slightly red-shifted (cf. Figure 10). Furthermore, a large number of photons have to be absorbed by the sol before a shift in the absorption spectrum is observed suggesting that a considerable number of electrons, rather than only one, have to be stored per particle to yield this effect. Finally, no spectral change is observed in alkaline suspensions where a negatively charged surface should result in overall negatively charged particles, evincing that the mechanism proposed in the case of CdS cannot simply be applied to ZnO. We prefer to use the MO picture introduced above to explain the data shown in Figure 10 (analogous results were also obtained in the absence of MV^{2+}). Illumination of the ZnO particles results in the oxidation of acetate and/or 2-propanol. Concurrently, the e_{CB}^- reduce all available electron acceptors such as chemisorbed dioxygen and methylviologen. Only a few micromoles of photons are necessary to deplete all relay compounds which originally promoted the visible emission, while the absorption band due to ZnO remained unchanged (curve -- in Figure 10). Subsequently, i.e., after the sol had been illuminated with 10 mM $h\nu$ (curve --- in Figure 10), excess electrons start to fill the lower MO's of the conduction band as indicated schematically in Figure 12. Hence, succeeding photogenerated electrons have to reach molecular orbitals of higher energy. Since in these small colloidal particles the density of MO's in the conduction band is relatively low, a net blue shift of the absorption spectrum is the expected result. The emission, on the other hand, occurs through transitions from the lower edge of the conduction band to the upper edge of the valence band in agreement with the absence of any blue shift of the UV fluorescence. Eventually, MV^{2+} is reduced to MV^0 via an intermediate $MV^{\bullet+}$ as indicated by the changes in the absorption spectra. However, it is not possible to decide whether the e_{CB}^- from the ZnO or the α-hydroxyalkyl radicals formed during the one-electron oxidation of 2-propanol lead to the observed formation of doubly reduced methylviologen.

Once O_2 is admitted to the system it reacts with the stored electrons and thereby restores the original spectral characteristics. Chemical reactions such as the oxidation of acetate and 2-propanol and the reduction of molecular oxygen resulted in a net chemical change in the colloidal suspension. We envisage that no spectral change would be observable under the given experimental conditions if we were able to produce zinc oxide colloids in the absence of electron donors since e^-/h^+ recombination should then be the main reaction pathway.

Even though the phrase "nonlinear optical effects" has been used to describe similar phenomena[23] a word of caution should be added at this point. Solid-state physics employs this term for completely reversible transient effects which, for example, occur in semiconductors that are irradiated with short light pulses of high intensity (e.g., laser pulses) the energy of which exceeds the bandgap energy. Hence a large number of e^-/h^+ pairs are generated which during their lifetime alter the optical absorption characteristics of the material in a nonlinear fashion.[65] However, as pointed out above, the observed spectral changes are, at least in our case, accompanied by permanent chemical changes within the illuminated system and can therefore not strictly be described by such a reversible model.

Acknowledgment. We gratefully acknowledge the financial support by the U.S. EPA (CR812356-01-0) and in particular we want to thank Dr. Marcia Dodge for her support. We appreciate extensive scientific discussions with Prof. Arnim Henglein (Hahn-Meitner Institute Berlin) who also supplied a preprint of his recent work[23] thereby stimulating our ideas concerning the nonlinear optical effects. We enjoyed a very pleasant collaboration with Prof. Douglas Magde (University of California, San Diego) during the fluorescence decay studies and like to thank him and Ms. Gale Rojas for their help. D.W.B. thanks the Hahn-Meitner Institut for granting him a leave of absence.

Registry No. MV^{2+}, 4685-14-7; MnO_4^-, 14333-13-2; $Cr_2O_7^{2-}$, 13907-47-6; Fe^{2+}, 15438-31-0; Cu^{2+}, 15158-11-9; Fe^{3+}, 20074-52-6; Cr^{3+}, 16065-83-1; Zn^{2+}, 23713-49-7; Co^{2+}, 22541-53-3; Ni^{2+}, 14701-22-5; Mn^{2+}, 16397-91-4; Ag^+, 14701-21-4; Li^+, 17341-24-1; ZnO, 1314-13-2.

(64) Albery, W. J.; Brown, G. T.; Darwent, J. R.; Saievar-Iranizad, E. *J. Chem. Soc., Faraday Trans. 1* **1985**, *81*, 1999.

(65) Chemla, D. S. *Nonlinear Optics: Materials and Devices; Proceedings in Physics*; Flytzanis, C., Oudar, J. L., Eds.; Springer Verlag: Berlin, 1986; Vol. 7, p 65.